Materials Transactions, Vol. 53, No. 1 (2012) pp. 81 to 86
Special Issue on Advanced Materials Science in Bulk Nanostructured Metals

Microstructure and Crystallographic Features of Martensite Transformed from Ultrafine-Grained Austenite in Fe–24Ni–0.3C Alloy

Akinobu Shibata*, Hamidreza Jafarian and Nobuhiro Tsuji

Department of Materials Science and Engineering, Kyoto University, Kyoto 606-8501, Japan

We studied microstructure and crystallographic features, especially orientation relationship, of martensite transformed from austenite with mean grain sizes ranging from 35 μm to 750 nm in an Fe–24Ni–0.3C alloy. The austenite structures with ultrafine or fine grains were fabricated through intense straining by accumulative roll-bonding process and subsequent annealing. The morphology of martensite transformed from the austenite with various grain sizes was all lenticular type. On the other hand, the martensite plate size decreased with the decrease in the austenite grain size. The orientation relationship of martensite transformed from coarse-grained austenite with mean grain size (d) of 35 μm changed depending on the location within martensite plate: i.e., it was Greninger–Troiano relationship at the center part of each martensite plate, while it changed to Kurdjumov–Sachs relationship near the interphase boundary. In contrast, the whole area of each martensite plate, transformed from fine-grained austenite ($d = 2.5$ μm) and ultrafine-grained austenite ($d = 750$ nm), satisfied Greninger–Troiano relationship. Furthermore, high density of dislocations and low angle boundaries within the ultrafine-grained austenite resulted in a large scatter of observed orientation relationship. [doi:10.2320/matertrans.MD201121]

(Received July 29, 2011; Accepted September 26, 2011; Published December 25, 2011)

Keywords: *steel, severe plastic deformation, ultrafine-grains, transformation, martensite, microstructure, orientation relationship*

1. Introduction

In recent years, ultrafine-grained materials having grain sizes smaller than 1 μm have been obtained through various severe plastic deformation processes.[1–6] The ultrafine-grained materials exhibit the unique properties[7] that have never been observed in conventional coarse-grained materials, as well as excellent mechanical properties.[8] Besides severe plastic deformation, another possible way to achieve finer microstructure and more superior mechanical properties is the combination of ultrafine-grained structure and phase transformation.[9] In the present study, we pay a special attention to martensitic transformation from ultrafine-grained austenite in steels, because martensite structure in steels has a very fine microstructure and exhibits high strength in its conventional state.

Several groups have studied martensitic transformation from ultrafine-grained austenite in steel.[10–13] Tadaki *et al.*[10,11] reported that the martensite transformation start temperature (Ms temperature) of austenitic powder particles having nanometer-sizes in Fe–Ni alloys was much lower than that in the bulky specimen with conventional grain size of austenite. It seems, however, that the martensitic transformation of powder particles with free surface is essentially different from that of bulky polycrystalline austenite grains. Takaki *et al.*[12] studied isothermal martensitic transformation behavior of austenitic stainless steels having fine grain sizes. Their results indicated that the isothermal martensitic transformation during holding at room temperature was suppressed when the grain size was smaller than 1 μm. Kitahara *et al.*[13] studied martensitic transformation from ultrafine-grained austenite in Fe–Ni alloy fabricated by severe plastic deformation, and reported that the Ms temperature of elongated ultrafine-grained austenite with mean grain thickness of 230 nm was about 40 K lower than that of the coarse-grained austenite.

*Corresponding author, E-mail: shibata.akinobu.5x@kyoto-u.ac.jp

Although several interesting phenomena described above have been reported, the mechanism of martensitic transformation of ultrafine-grained austenite has not yet been systematically understood. The present study investigates microstructural and crystallographic features, especially orientation relationship with respect to austenite, of martensite transformed from the ultrafine-grained polycrystalline austenite fabricated by severe plastic deformation.

2. Experimental Procedure

An Fe–24Ni–0.3C (mass%) alloy, whose Ms temperature is 245 K and below room temperature, was used in the present study. Table 1 shows the detailed chemical composition of the alloy. A cast ingot of the alloy was hot-rolled and then cold-rolled to make a sheet with thickness of 1 mm. The sheet was austenitized at 1173 K for 3.6 ks. The austenitized specimen had a fully austenite structure with mean grain size of 35 μm. The austenitized specimens were provided to accumulative roll-bonding (ARB) process, which is one of the severe plastic deformation processes, to obtain ultrafine-grained structure of austenite. The principle of the ARB process has been reported previously.[5,6] Two pieces of the austenitized sheets were stacked to be 2 mm in thickness after contact surfaces were degreased and wire-brushed, and held in a box furnace at 873 K for 0.6 ks, at which austenite phase of the used alloy is stable, in order to prevent the formation of deformation-induced martensite during rolling process. Then the stacked sheet was rolled by 50% reduction in one pass at 873 K, and immediately water-quenched. The rolling in the ARB process is not only a deformation process but also a bonding process (roll-bonding). The roll-bonded sheet was

Table 1 Chemical composition of the alloy used (mass%).

C	Si	Mn	P	S	Ni	O	N	Fe
0.29	0.01	0.07	<0.005	<0.0005	24.09	0.0008	0.0006	Bal.

cut into two, stacked to have the initial dimension (2 mm in thickness), and roll-bonded again. We continued the procedures up to 6 cycles, corresponding to a total reduction in thickness of 98.4%, i.e., an equivalent strain of 4.8. The 6-cycle ARB processed specimens were subsequently annealed at 873 K for 1.8 ks to obtain fully recrystallized and fine-grained austenite. The specimens at various stages of the process were cooled in liquid nitrogen temperature to cause martensitic transformation.

The Ms temperature was measured by a differential scanning calorimetry at a cooling rate of $4\,K\,min^{-1}$. Microstructures of the specimens were observed by optical microscopy, scanning electron microscopy (SEM) using a field-emission type SEM (FEI: XL30S-FEG), and transmission electron microscopy (TEM, Philips: CM200FEG). For the optical microscopy and SEM observations, the specimens were mechanically polished and then electrolytically polished in a solution of 90% CH_3COOH + 10% $HClO_4$. The thin-foil specimens for the TEM observation were prepared by twin-jet electrolytic polishing in the same solution as described above. The crystal orientations of the specimens were measured by electron backscattering diffraction (EBSD) analyzer in SEM operated at 15 kV using the TSL OIM Data Collection program, and measured orientations were analyzed with the TSL OIM Analysis program.

For martensitic transformation in iron-based alloys, three kinds of orientation relationships have been reported; Kurdjumov–Sachs (K–S) relationship ($\{111\}_A$ // $\{011\}_M$, $\langle 101\rangle_A$ // $\langle 111\rangle_M$), Nishiyama–Wassermann (N–W) relationship ($\{111\}_A$ // $\{011\}_M$, $\langle 112\rangle_A$ // $\langle 011\rangle_M$), and Greninger–Troiano (G–T) relationship ($\{111\}_A$ 1° from $\{011\}_M$, $\langle 101\rangle_A$ 2.5° from $\langle 111\rangle_M$), where the subscripts A and M denote austenite and martensite, respectively. The G–T relationship is halfway between the K–S and N–W relationships. In order to describe the orientation relationship of martensite with respect to austenite, the measured orientations of austenite and martensite were indexed with respect to the standard K–S variant: $(111)_A$ // $(011)_M$, $[\bar{1}01]_A$ // $[\bar{1}\bar{1}1]_M$. Then, we plotted the $[\bar{1}\bar{1}1]_M$ directions of martensite on a standard $[001]_A$ stereographic projection; in other words, the directions of austenite parallel to $[\bar{1}\bar{1}1]_M$ directions of martensite were plotted on a standard $[001]_A$ stereographic projection. The $[\bar{1}\bar{1}1]_M$ directions of martensite based on the coordinate system fixed in austenite were calculated from the orientation matrices of martensite and austenite obtained from the EBSD orientation map.

3. Results and Discussion

3.1 Microstructures of transformed martensite

Figure 1 shows boundary maps of austenite obtained by EBSD measurement; (a) after the first austenitization at 1173 K, and (b) after 6-cycle ARB processing and subsequent annealing at 873 K for 1.8 ks. The low angle boundaries with misorientation of 2–15° are drawn in gray lines, while the high angle boundaries with misorientation above 15° are drawn in black lines in Fig. 1. The austenite after austenitization at 1173 K [Fig. 1(a)] and that after the ARB plus annealing [Fig. 1(b)] have equiaxed grains, and mean grain sizes measured by line interception method are 35 and 2.5 μm, respectively. Hereafter, we refer to these austenites in Figs. 1(a) and 1(b) as "coarse-grained austenite" and "fine-grained austenite", respectively. Figure 2(a) is an EBSD boundary map of the austenite after 6-cycle ARB processing. The austenite after 6-cycle ARB processing exhibits lamellar structure elongated along the rolling direction (RD) of the sheet. The average interval of high angle boundaries along the normal direction (ND) of the sheet is 750 nm. We refer the austenite after 6-cycle ARB processing [Fig. 2(a)] as "ultrafine-grained austenite". Figure 2(b) is a Kernel average misorientation map of the ultrafine-grained austenite, where color of each point expresses the average misorientation between the data point and all of its neighbors. Local orientation within the grains is quite inhomogeneous. Figures 2(c) and 2(d) are a TEM image and corresponding misorientation map of the ultrafine-grained austenite. High density of dislocations and low angle boundaries within lamellar structures are observed. The large local misorientation inside the elongated grain shown in Fig. 2(b) is attributed to the high density of dislocations and low angle boundaries shown in Figs. 2(c) and 2(d). Accordingly, we can conclude that the ultrafine-grained austenite fabricated by the ARB process is a kind of deformation microstructure formed through the grain subdivision process.[14,15)]

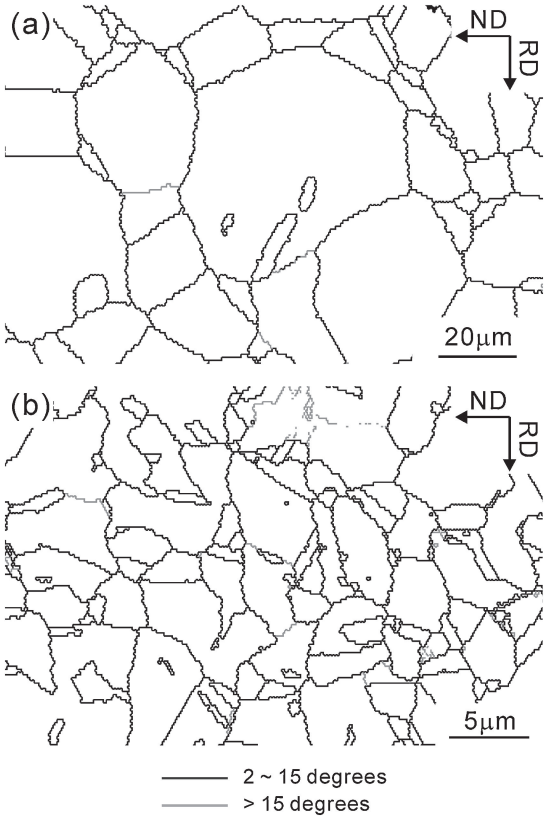

Fig. 1 Boundary maps of austenite obtained by EBSD measurements; (a) the coarse-grained austenite (after austenitized at 1173 K for 1.8 ks), (b) the fine-grained austenite (after 6-cycle ARB processing and subsequent annealing at 873 K for 1.8 ks).

The Ms temperatures of the coarse-grained austenite, the fine-grained austenite, and the ultrafine-grained austenite were 245, 228, and 243 K, respectively. It was reported that Ms temperature decreases with decrease of austenite grain

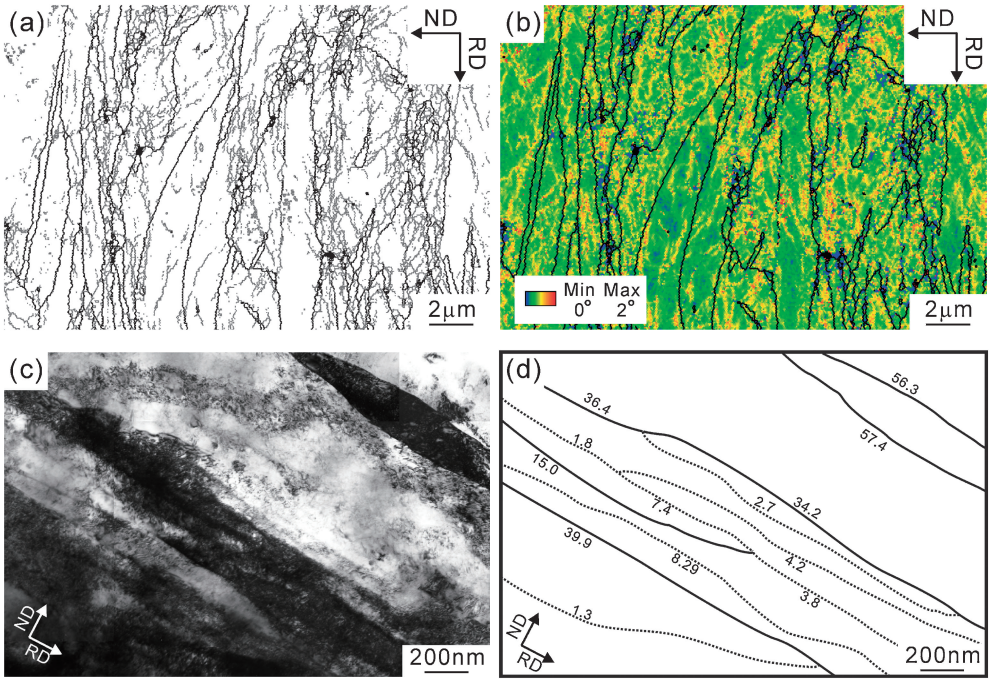

Fig. 2 (a), (b) Boundary map and corresponding Kernel average misorientation map of the ultrafine-grained austenite (after 6-cycle ARB processing) obtained by EBSD measurement; (c), (d) TEM image and corresponding misorientation map of the ultrafine-grained austenite.

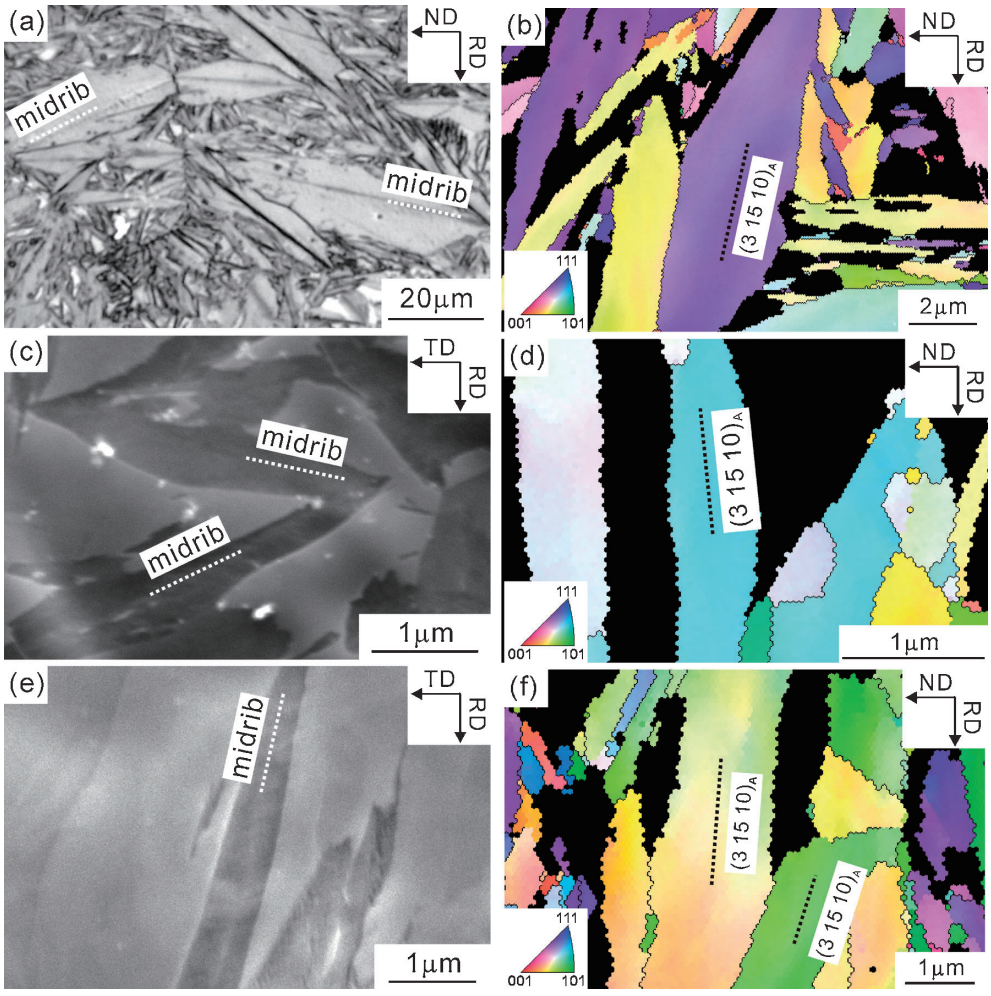

Fig. 3 (a), (b) Optical microscopy image and EBSD orientation map of martensite transformed from the coarse-grained austenite ($Ms = 245$ K); (c), (d) SEM image and EBSD orientation map of martensite transformed from the fine-grained austenite ($Ms = 228$ K); (e), (f) SEM image and EBSD orientation map of martensite transformed from the ultrafine-grained austenite ($Ms = 243$ K).

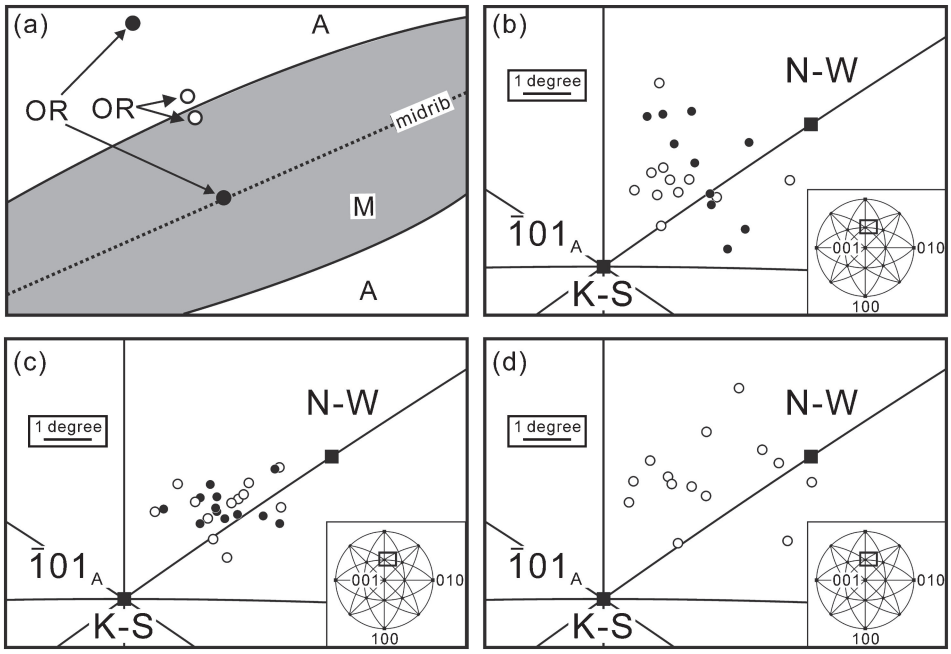

Fig. 4 (a) Schematic illustration showing the measured positions of orientations of martensite and austenite. (b)–(d) Standard $[001]_A$ stereographic projections around $[\bar{1}01]_A$ axis showing the $[\bar{1}\bar{1}1]_M$ directions of martensite (open and solid circles) transformed from (b) the coarse-grained austenite, (c) the fine-grained austenite, and (d) the ultrafine-grained austenite. The ideal $[\bar{1}\bar{1}1]_M$ directions of martensite for the exact K–S and N–W relationships are also indicated as solid squares.

size.[13,16] However, the Ms temperature of the ultrafine-grained austenite was relatively high even though the grain size of the ultrafine-grained austenite is significantly small when compared with the coarse-grained and fine-grained austenites. Because dislocation can act as a nucleation site for martensitic transformation,[17] the relatively high Ms temperature of the ultrafine-grained austenite was attributable to the existence of high density of dislocations and low angle boundaries inside the austenite grain as shown in Figs. 2(c) and 2(d).

Figure 3(a) is an optical microscopy image showing the morphology of martensite transformed from the coarse-grained austenite ($Ms = 245$ K). The morphology of martensite is plate type with smoothly curved interphase boundaries. We can also observe midrib in the middle of martensite plate clearly. Figure 3(b) is an EBSD orientation map of martensite transformed from the coarse-grained austenite, where the colors express the orientation parallel to the transverse direction (TD) of the sheet. The trace of midrib corresponds to $(3\ 15\ 10)_A$ plane. It is well known that lenticular martensite contains midrib of which habit plane is close to $(3\ 15\ 10)_A$.[18] Figures 3(c)–3(f) are SEM images and EBSD orientation maps of martensite transformed from the fine-grained austenite ($Ms = 228$ K) and the ultrafine-grained austenite ($Ms = 243$ K). We can also observe midribs inside the martensite plates in Figs. 3(c) and 3(e). In addition, the traces of the midribs correspond to $(3\ 15\ 10)_A$, as shown in Figs. 3(d) and 3(f). On this basis, we can conclude that the martensite transformed from the coarse-grained austenite, the fine-grained austenite, and the ultrafine-grained austenite are all lenticular type. It was reported that Ms temperature greatly affects the martensite morphology.[19] Almost the same Ms temperature of the coarse-grained austenite, the fine-grained austenite, and the ultrafine-grained austenite resulted in the formation of lenticular martensite irrespective of austenite grain size.

With decrease in the austenite grain size, martensite plate size also decreased. The mean sizes of the martensite plates transformed from the coarse-grained austenite, the fine-grained austenite, and the ultrafine-grained austenite, measured by line interception method, are 3.7 μm, 410 nm, and 260 nm, respectively. The decrease in martensite plate size depending on the austenite grain size is due to the fact that martensite plates can not grow across austenite grain boundaries.

3.2 Orientation relationship of martensite with respect to austenite

According to the previous studies,[20,21] the local orientation of austenite changed in the vicinity of interphase boundary, because dislocations accommodating the transformation strain were accumulated nearby the interphase boundaries. Thus, the orientation change in the surrounding austenite should be taken into account when considering the orientation relationship. As shown in a schematic illustration of Fig. 4(a), the orientation relationship at the middle part of martensite plate was obtained using the orientation of austenite far from the interphase boundary (solid circles), as we can assume that the orientation of austenite before martensitic transformation is maintained in the region far from interphase boundary which is not plastically deformed during martensite transformation. On the other hand, the orientation relationship in the vicinity of interphase boundary was obtained using the orientation of austenite just beside the interphase boundary (open circles). Figure 4(b) is the enlarged region around $[\bar{1}01]_A$ of standard $[001]_A$ stereographic projection showing the orientation relationship of martensite transformed from the coarse-grained austenite.

The points express the experimentally measured $[\bar{1}\bar{1}1]_M$ directions of martensite picked up from many different martensite plates, and solid and open circles represent the orientation relationship at the middle part of martensite plate and that in the vicinity of interphase boundary, respectively. The ideal $[\bar{1}\bar{1}1]_M$ directions of martensite for the exact K–S and N–W relationships are also indicated as solid squares. We find that the $[\bar{1}\bar{1}1]_M$ directions of martensite at the middle part of martensite plate are distributed around the area between the K–S and N–W relationships [Fig. 4(b)], indicating that the middle part of martensite plate satisfies the G–T relationship with respect to austenite. On the other hand, the $[\bar{1}\bar{1}1]_M$ directions of martensite in the vicinity of interphase boundary are close to that of K–S relationship. This indicates that the orientation relationship of lenticular martensite changed from the G–T to K–S relationships during growth. This inhomogeneous orientation relationship inside the martensite plate was also reported in the previous work.[20] Figure 4(c) shows the orientation relationship of martensite transformed from the fine-grained austenite. In contrast to Fig. 4(b), the $[\bar{1}\bar{1}1]_M$ directions at the middle part of the martensite plate and that just beside the interphase boundary were all plotted in the middle of the K–S and N–W relationships in Fig. 4(c). This suggests that the whole area in the martensite plates transformed from the fine-grained austenite satisfies the G–T relationship with respect to austenite.

As shown in Fig. 4(b), the orientation relationship of the lenticular martensite transformed from the coarse-grained austenite changed from the G–T to K–S relationships as approaching from the middle part of the martensite plates to the interphase boundaries. As described above, the size of the martensite plates transformed from the fine-grained austenite is much smaller than that transformed from the coarse-grained austenite. Accordingly, we consider that the martensite transformed from the fine-grained austenite did not grow enough to change the orientation relationship from the G–T to K–S relationships, resulting that the whole area in the martensite plates satisfies the G–T relationship [Fig. 4(c)].

The orientation relationship of martensite transformed from the ultrafine-grained austenite is shown in Fig. 4(d). In Fig. 4(d), we plotted only the orientation relationship just beside the interphase boundary, because large local orientation distribution inside the ultrafine-grained austenite [Fig. 2(b)] made it very difficult to know the exact orientation of austenite before transformation. Similar to Fig. 4(c), the $[\bar{1}\bar{1}1]_M$ directions of martensite are located in between the K–S and N–W relationships, indicating that the martensite holds the G–T relationship with respect to austenite. This is also attributed to the small size of martensite plate transformed from the ultrafine-grained austenite. Compared with Figs. 4(b) and 4(c), however, the $[\bar{1}\bar{1}1]_M$ directions of martensite in Fig. 4(d) are significantly scattered between different martensite plates. Previous papers[21,22] demonstrated that martensite inherits dislocations or dislocation boundaries in austenite during transformation. Accordingly, we consider that high density of dislocations and low angle boundaries inside the austenite grains reduced the coherency between martensite and austenite, resulting in the large scatter of observed orientation relationships.

4. Summary

The present paper reported the microstructure and orientation relationship of martensite transformed from austenite with different grain sizes; the coarse-grained austenite (grain size of 35 μm), the fine-grained austenite (grain size of 2.5 μm), and the ultrafine-grained austenite (grain size of 750 nm). The conclusions are summarized as follows;

(1) The morphology of martensite transformed from the austenite with grain sizes ranging from 35 μm to 750 nm was all lenticular type containing midrib. With decrease in the austenite grain size, the size of martensite plate also decreased.

(2) The orientation relationship of martensite transformed from the coarse-grained austenite was the G–T relationship at the middle part of martensite plate, but shifted to the K–S relationship as approaching the interphase boundary. In contrast, the whole area in the martensite plates transformed from the fine-grained austenite satisfied the G–T relationship. This was attributed to the small size of martensite plate transformed from the fine-grained austenite.

(3) The orientation relationship of martensite transformed from the ultrafine-grained austenite was the G–T relationship, but the observed orientation relationships were significantly scattered between different martensite plates. We considered that the existence of high density of dislocations and low angle boundaries inside the austenite grains reduced the coherency between martensite and austenite, resulting in the large scatter of observed orientation relationships.

Acknowledgment

This study was financially supported by the Grant-in-Aid for Scientific Research Innovative Area, “Bulk Nanostructured Metals” through the Ministry of Education, Culture, Sports, Science and Technology (MEXT), Japan (contact No. 22102002), and the support is gratefully appreciated.

REFERENCES

1) R. Z. Valiev, A. V. Korznikov and R. R. Mulyukov: Mater. Sci. Eng. A **168** (1993) 141–148.
2) V. M. Segal: Mater. Sci. Eng. A **197** (1995) 157–164.
3) Y. Ma, M. Furukawa, Z. Horita, M. Nemoto, R. Z. Valiev and T. G. Langdon: Mater. Trans. **37** (1996) 336–339.
4) R. Z. Valiev, R. K. Islamgaliev and I. V. Alecandrov: Prog. Mater. Sci. **45** (2000) 103–189.
5) N. Tsuji, Y. Saito, H. Utsunomiya and S. Tanigawa: Scr. Mater. **40** (1999) 795–800.
6) N. Tsuji, Y. Sato, S. H. Lee and Y. Minamino: Adv. Eng. Mater. **5** (2003) 338–344.
7) X. Huang, N. Hansen and N. Tsuji: Science **312** (2006) 249–251.
8) R. Z. Valiev: Nature Mater. **3** (2004) 511–516.
9) N. Tsuji and T. Maki: Scr. Mater. **60** (2009) 1044–1049.
10) T. Tadaki, Y. Murai, A. Koreeda, Y. Nakata and Y. Hirotsu: Mater. Sci. Eng. A **217–218** (1996) 235–238.
11) K. Asaka, Y. Hirotsu and T. Tadaki: Mater. Sci. Eng. A **273–275** (1999) 262–265.
12) S. Takaki, K. Fukunaga, J. Syarif and T. Tsuchiyama: Mater. Trans. **45** (2004) 2245–2251.

13) H. Kitahara, N. Tsuji and Y. Minamino: Mater. Sci. Eng. A **438–440** (2006) 233–236.
14) N. Hansen and D. Juul Jensen: Philos. Trans. R. Soc. London A **357** (1999) 1447–1469.
15) N. Hansen: Metall. Mater. Trans. A **32A** (2001) 2917–2935.
16) M. Umemoto and W. Owen: Metall. Trans. **5** (1974) 2041–2046.
17) G. B. Olson and M. Cohen: Metall. Trans. A **7A** (1976) 1905–1914.
18) P. L. Patterson and C. M. Wayman: Acta Metall. **12** (1964) 1306–1311.
19) T. Maki, S. Shimooka, S. Fujiwara and I. Tamura: Trans. JIM **16** (1975) 35–41.
20) A. Shibata, S. Morito, T. Furuhara and T. Maki: Scr. Mater. **53** (2005) 597–602.
21) A. Shibata, S. Morito, T. Furuhara and T. Maki: Acta Mater. **57** (2009) 483–492.
22) T. Maki and C. M. Wayman: Metall. Trans. A **7A** (1976) 1511–1518.